BİTLİS EREN UNIVERSITY

JOURNAL OF SCIENCE AND TECHNOLOGY

E-ISSN: 2146-7706

MODELING AND COMPREHENSIVE STRATEGIC INTERVENTION ANALYSIS FOR HEPATITIS A AND E INFECTIONS: A PARADIGM SHIFT IN PUBLIC HEALTH DYNAMICS

Adedapo Chris Loyinmi

Tai Solarin University of Education, Department of Mathematics, Ogun State, Nigeria
loyinmiac@tasued.edu.ng

KEYWORDS

Hepatitis A & E
Optimal control Strategies
Public health interventions
Sensitivity analysis
Mathematical modelling

ARTICLE INFO

Research Article
Doi
10.17678/beuscitech.1573256

Received	October 24, 2024
Revised	January 19, 2025
Accepted	February 21, 2025
Year	2025
Volume	15
Issue	1
Pages	1-36

ABSTRACT

Infectious diseases like Hepatitis A and E pose substantial challenges to public health globally, necessitating innovative strategies that combine mathematical modelling with strategic intervention analysis. This study introduces a comprehensive mathematical model designed to encapsulate the complex dynamics of Hepatitis A and E infections, including susceptibility, vaccination, latent and acute phases, treatment, and recovery.

A thorough quantitative analysis was performed, encompassing the non-negativity and boundedness of solutions, the disease-free equilibrium, and the basic reproductive ratio. Stability analyses provided critical insights into the local and global dynamics of the model, essential for understanding the conditions under which the diseases persist or are controlled.

Sensitivity analysis highlighted key parameters driving disease transmission, aiding in the development of targeted intervention strategies. Utilizing optimal control theory, innovative intervention frameworks were formulated to optimize vaccination campaigns, allocate treatment resources efficiently, implement health education programs, and enhance sanitation measures. Numerical simulations further demonstrated the effectiveness of these interventions, showcasing their influence on population dynamics, disease prevalence, and environmental contamination.

1 INTRODUCTION

The historical trajectory of hepatitis, spanning from ancient civilizations to modern scientific discoveries, reflects a complex interplay between human behavior, societal conditions, and viral pathogens. Millennia ago, descriptions of clinical syndromes resembling hepatitis can be traced back to Sumerian medical texts, highlighting the enduring presence of this disease throughout human history. Hippocrates' observations of "epidemic jaundice" further underscored the recognition of hepatitis-like illnesses in antiquity. During subsequent centuries, particularly in the Middle Ages, rudimentary understanding of jaundice transmission emerged, exemplified by Pope Zacharias' quarantine measures [1-4]. However, it wasn't until the 20th century, amid the upheavals of global conflicts, that significant strides were made in elucidating the viral etiology of hepatitis. Pioneering experiments during World War II revealed distinct subtypes of viral hepatitis, paving the way for the identification of hepatitis A and hepatitis B. By the late 1970s, the emergence of hepatitis C as a distinct pathogen underscored the complexity of viral hepatitis. The discovery of hepatitis E virus (HEV) further expanded our understanding, particularly in regions where hepatitis A was traditionally assumed to be the primary cause of waterborne outbreaks [5-8]. The pivotal moment came when Russian virologist Mikhail Balayan's self-experimentation led to the identification of HEV, shedding light on a previously unrecognized form of viral hepatitis. From a virological perspective, hepatitis A virus (HAV) and HEV belong to different families and exhibit distinct genetic characteristics [9-18]. Despite their differences, both viruses share a remarkable ability to survive in the environment due to their non-enveloped structure, facilitating transmission through contaminated food and water sources. This underscores the importance of sanitation measures in preventing hepatitis outbreaks. Epidemiologically, HAV and HEV display contrasting patterns of transmission and geographic distribution. While HAV primarily spreads through fecal-oral routes, HEV transmission encompasses zoonotic and waterborne routes, with variations in prevalence across different regions. Understanding these transmission dynamics is crucial for implementing targeted prevention strategies. Clinically, both HAV and HEV can cause acute hepatitis with varying degrees of severity, although chronic infection is rare with HAV. The clinical presentation of hepatitis A and E can

overlap, but distinct features may aid in differential diagnosis [17-21]. Moreover, the emergence of extra hepatic manifestations further complicates the clinical picture, highlighting the multisystem nature of these infections. Diagnosing hepatitis, particularly HEV infection, presents challenges due to limited awareness among clinicians and variability in testing availability and accuracy. Treatment options for acute hepatitis A and E are primarily supportive, with ribavirin showing efficacy in selected cases of severe acute hepatitis E. In chronic HEV infection, reduction of immunosuppression and antiviral therapy with ribavirin are considered, emphasizing the importance of tailored management approaches. Prevention remains the cornerstone of hepatitis control efforts, encompassing measures such as vaccination, sanitation improvements, and public health interventions. Vaccination against HAV and the availability of an HEV vaccine in certain regions offer promising avenues for disease prevention [22-32].

The seminal mathematical framework for analyzing the propagation of infectious diseases was spearheaded by Bernoulli in 1760. Its primary objective was to evaluate the impact of variolation, an early technique akin to smallpox vaccination, on life-tables utilized in actuarial calculations. Mathematical models play an indispensable role in scientific and medical spheres, enabling the interpretation of outcomes, formulation of hypotheses, design of experiments, derivation of diagnoses from clinical presentations and test results, and provision of guidance for decision-making processes [1], [16], [33-40]. Mathematical representation of models allows for meticulous analysis, enabling quantitative forecasts regarding disease trends and intervention impacts. Increasingly, the utilization of mathematical frameworks in elucidating the dynamics of infectious disease propagation holds significant prominence in the formulation of public health protocols. Notable applications encompass the management of the foot-and-mouth disease outbreak in the UK during 2001, addressing episodes of severe acute respiratory syndrome (SARS) and Middle East respiratory syndrome coronavirus (MERS-CoV), devising strategic approaches for controlling tuberculosis (TB), human immunodeficiency virus (HIV), and sexually transmitted infections (STIs), as well as crafting vaccination policies, enhancing preparedness for pandemic influenza, planning responses to bioterrorism threats, strategizing intervention trials, assessing the efficacy of interventions, enriching comprehension of disease progression, and

investigating fundamental principles governing disease control [31-34], [39-42]. Infectious disease epidemiology is inherently interdisciplinary as infection transmission within a populace is influenced not only by the biological attributes of the infectious agent and its host, but also by host (and vector, where applicable) contact patterns, environmental factors, and human utilization of healthcare services and response to public health measures, among other factors. Mathematical modeling serves to delineate the intricate interplay among these factors and enables integration of data from diverse disciplines, including social sciences. Crucially, models ought not to be enigmatic constructs but should be lucidly expounded to enable assessment of model validity and data utilization by non-modelers. Modeling embodies the process of formalizing conceptualizations of a system, aimed at enhancing clarity; nevertheless, infectious disease transmission dynamics typically exhibit inherent complexity [3], [5], [7], [38-46].

To gain deeper insights into the epidemiological characteristics of Hepatitis A and E, researchers employ sophisticated mathematical modeling techniques akin to those utilized in studying diseases like diphtheria, pertussis, and influenza. This analytical approach, widely employed in infectious disease epidemiology, enables a systematic exploration of the intricate patterns of transmission within populations. Just as mathematical models have been instrumental in elucidating transmission dynamics of various infectious diseases, from COVID-19 to Lassa fever, we introduce a comprehensive model tailored specifically to understand the transmission dynamics of Hepatitis A and E viruses [2], [3], [7], [46-50].

Infectious diseases, such as Hepatitis A and E, present significant challenges to public health worldwide. Addressing these challenges requires innovative approaches integrating mathematical modeling and strategic intervention analysis, hence this research study holds significant implications for public health epidemiology by providing a comprehensive framework for understanding and controlling Hepatitis A and E infections. Through mathematical modeling and quantitative analysis, the proposed model elucidates the dynamics of transmission, the impact of interventions such as vaccination and treatment, and the effectiveness of sanitation measures. By identifying key parameters and evaluating their sensitivity, the study offers valuable insights into optimal control strategies for taming disease burden. Findings will further contribute to evidence-based decision-

making in disease prevention and control, aiding policymakers and healthcare professionals in implementing targeted interventions to reduce Hepatitis A and E transmission and improve population health outcomes.

The proposed mathematical model and use of optimal control theory offer a unique and comprehensive framework for analyzing the dynamics of Hepatitis A and E infections. Unlike traditional SIRS models, this study integrates critical real-world factors such as pathogen shedding into water and food supplies, the impact of sanitation measures, and the interplay between vaccination, treatment, and environmental contamination. By leveraging Pontryagin's Maximum Principle, the research innovatively optimizes intervention strategies, providing a targeted approach to controlling disease transmission. Furthermore, this model advances existing literature by focusing specifically on the dual dynamics of Hepatitis A and E, offering insights that were previously underexplored in public health modeling. Through sensitivity analysis and numerical simulations, the study identifies and prioritizes key parameters influencing disease spread, paving the way for more effective, evidence-based intervention strategies.

2 MATERIALS AND METHOD

2.1 Model Description

We have adapted and modified a model that bears resemblance to the SIRS (Susceptible-Infectious-Recovered-Susceptible) model (Figure 1). This model comprises the following classes:

1. Susceptible (S): This class represents individuals who are susceptible to the infection and have not yet been exposed to it.

2. Vaccinated Class (V): Individuals in this class have received a vaccine before being exposed to the infection, providing them with a level of immunity.

3. Latent Individuals (L): This class includes individuals who have been exposed to the infection but have not yet developed clinical symptoms. They are asymptomatic carriers capable of transmitting the virus.

4. Acute Individuals (A): Individuals in this class have been exposed to the infection and are showing clinical symptoms. They are actively infected and capable of transmitting the virus to others.

5. Treated Acute (T): Acutely infected individuals undergoing treatment aimed at reducing their infectiousness and promoting their recovery.

6. Recovered Individuals (R): This class represents individuals who have recovered from the infection and have developed immunity against it.

This model provides a comprehensive framework for examining the dynamics of Hepatitis A and E infection, including vaccination and treatment effects across different stages of the infection cycle.

The force infection is given as

$$\omega = \rho_1 A + \rho_2 P \tag{1}$$

The model incorporates various parameters to describe the dynamics of the infection. These parameters are detailed in Table 1. Additionally, the flow map illustrating the progression of the infection is depicted in Figure 2.

***Table 1**. Explanation of the parameters utilized in the model.*

Parameters	Description
Γ	Rate of entry into the susceptible population
ϕ	Fraction of the population vaccinated
σ	Rate of vaccination among susceptible individuals
ω	Force of infection for Hepatitis A and E
a	Proportion of acute cases recovering without treatment
γ	Rate of treatment among acute cases
θ_1	Rate of recovery among treated individuals
η	Rate of pathogen mortality due to sanitation measures
δ_1	Rate of pathogen excretion into water or food supply by infectious individuals in the acute stage
δ_2	Rate of pathogen excretion into water or food supply by treated individuals
μ	Rate of natural mortality
μ_p	Rate of Hepatitis A and E disease induction
ξ	Maximum per capita growth rate of Hepatitis A and E pathogens
τ	Rate of progression from latent stage to infected stage
θ_2	Recovery rate of treated individuals

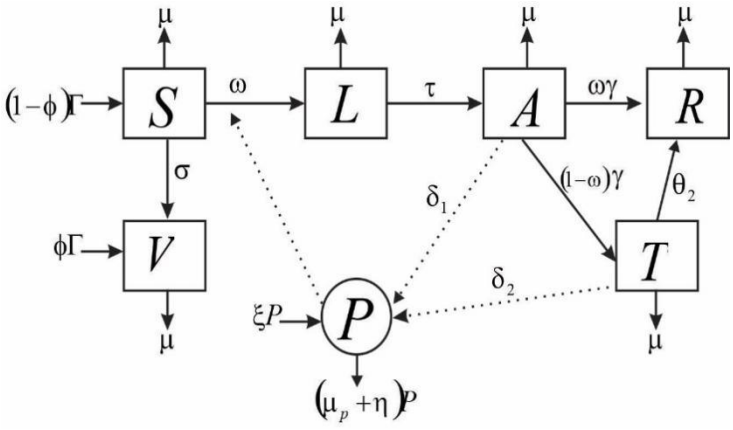

Figure 1. *Schematic diagram interaction of each compartment.*

2.2 The Equations of the Model

From the aforementioned description, the system of equations takes the following form:

$$\left.\begin{aligned}
\frac{dS}{dt} &= (1-\phi)\Gamma - (\omega+\sigma+\mu)S \\
\frac{dV}{dt} &= \phi\Gamma + \sigma S - \mu V \\
\frac{dL}{dt} &= \omega S - (\tau+\mu)L \\
\frac{dA}{dt} &= \tau L - (a\gamma + (1-a)\gamma + \mu + \delta_1)A \\
\frac{dT}{dt} &= (1-a)\gamma A - (\theta_2 + \mu + \delta_2)T \\
\frac{dR}{dt} &= a\gamma A + \theta_2 T - \mu R \\
\frac{dP}{dt} &= \delta_1 A + \delta_2 R - (\mu_p + \eta - \xi)P
\end{aligned}\right\} \quad \textbf{(2)}$$

2.3 A Comprehensive Investigation into the Model's Quantitative Attributes

2.3.1 Non-negativity and boundedness of solution

The system (2) can be divided into two separate components: one delineating the human population N_H and the other describing the viral concentration in the surrounding environment, particularly in food and water reservoirs N_P.

The differential equation for the human population $N_H = S+V+L+A+T+R$ is as follows:

$$\frac{dN_H}{dt} = \frac{dS}{dt} + \frac{dV}{dt} + \frac{dL}{dt} + \frac{dA}{dt} + \frac{dT}{dt} + \frac{dR}{dt} \quad \textbf{(3)}$$

Through the substitution of the model system represented by equation (2) into equation (3) and subsequent elimination, we achieve the following result:

$$\frac{dN}{dt} = (1-\phi)\Gamma - \mu N + \delta(A+T) \quad \textbf{(4)}$$

Theorem 1: Let (S,V,L,A,T,R) be the solution of equation (1) with the initial conditions in a biologically feasible region Φ with: $\Phi = (S,V,L,A,T,R) \in R_+^6 : N_H \leq \frac{\Gamma}{\mu}$

Then Φ is non-negative invariant.

So, Where $\delta = 0$ at DFE, equation (4) becomes

$$\frac{dN_H}{dt} = \Gamma - \mu N \quad \textbf{(5)}$$

By employing the integrating factor method to solve equation (5), we acquire:

$$\therefore \lim_{t\to\infty} N_H(t) \leq \frac{\Gamma}{\mu} \quad \textbf{(6)}$$

We conducted a verification process to ensure the non-negativity and boundedness of the solution, thereby affirming the physical and epidemiological plausibility of the model's predictions. This verification safeguards against scenarios where the number of individuals within a compartment becomes negative, maintaining the integrity of the model's outcomes. Additionally, we confirmed that the Hepatitis A and E model does not exhibit unbounded growth, as its values are constrained within defined limits. This boundedness feature prevents unrealistic scenarios wherein the disease proliferates uncontrollably, ensuring that the predictions remain within attainable levels throughout the transmission process.

2.3.2 Disease- free steady-state

In this context, we examine the dynamics of the mathematical model under conditions where the disease is absent, and the population remains unaffected by new disease cases. It is important to emphasize that despite the absence of the disease, every individual within the population is considered susceptible, indicating their vulnerability to potential infections.

So, then, $S^0 \neq 0$,

For $S^0 \neq 0, V^0 = 0, L^0 = 0, A^0 = 0, T^0 = 0, R^0 = 0, P^0 = 0$,

Consequently, the set of equations delineated in the model (2) $\Gamma - \mu S^0 = 0$.

And this gives;

$$S^o = \frac{\Gamma}{\mu} \tag{7}$$

This produces the asymptotic state devoid of disease among the individuals, characterized by:

$$E^0 = \left(S^0, V^0, L^0, A^0, R^0, T^0, P^0\right) = \left(\frac{\Gamma}{\mu}, 0,0,0,0,0,0\right) \tag{8}$$

2.3.3 Basic reproductive ratio

In this analysis, we delineate the pivotal epidemiological parameter utilized for quantifying the potential dissemination of the ailment across the populace. It is imperative to acknowledge that this metric denotes the mean count of subsequent infections induced by a solitary infective entity within an entirely susceptible population. This parameter assumes critical importance in comprehending the intricacies inherent in the transmission dynamics of Hepatitis A and E, as well as in appraising the efficacy of containment methodologies.

The fundamental parameter representing the propagation potential within the model's system equation (2) is determined through the application of the next generation matrix method as elucidated by Diekmann and Heesterbeek.

Using

$$R_n = \rho(AB^{-1})$$

Consider the infected compartments in the model (2) are L, A and P.

The terminology denoting new infections and transitions in system (1) are expressed as follows;

In the model (2), the compartments representing infected individuals are denoted as L, A and P.

The terms describing new infections and transitions in system (1) are expressed as follows:

$$A = \begin{pmatrix} (\rho_1 A + \rho_2 P)S \\ 0 \\ 0 \end{pmatrix} \quad \textbf{(9)}$$

And

$$B = \begin{pmatrix} (\tau + \mu)L \\ -\tau L + (a\gamma + (1-a)\gamma + \mu + \delta_1)A \\ -\delta_1 A - \delta_2 R + (\mu_p + \eta - \xi)P \end{pmatrix} \quad \textbf{(10)}$$

Let $L = g_{1,} A = g_{2,} P = g_3$

$$F_* = \begin{bmatrix} \frac{dg_1}{dL} & \frac{dg_1}{dA} & \frac{dg_1}{dP} \\ \frac{dg_2}{dL} & \frac{dg_2}{dA} & \frac{dg_2}{dP} \\ \frac{dg_3}{dL} & \frac{dg_3}{dA} & \frac{dg_3}{dP} \end{bmatrix} \quad \textbf{(11)}$$

Upon solving equation (11), we obtain:

$$A_* = \begin{bmatrix} 0 & \rho_1 S & \rho_2 S \\ 0 & 0 & 0 \\ 0 & 0 & 0 \end{bmatrix} \quad \textbf{(12)}$$

Likewise,

$$B_* = \begin{bmatrix} (\tau+\mu) & 0 & 0 \\ -\tau & (a\gamma+(1-a)\gamma+\mu+\delta_1) & 0 \\ 0 & -\delta_1 & (\mu_p+\eta-\xi) \end{bmatrix} \quad \textbf{(13)}$$

Let $a=(\tau+\mu)$; $b=-\tau$; $c=(a\gamma+(1-a)\gamma+\mu+\delta_1)$; $d=-\delta_1$; and $e=(\mu_p+\eta-\xi)$

Now, we try to find the $B_*^{-1}=\frac{1}{|B_*|}adjB_*$

$$B_*^{-1} = \begin{bmatrix} \frac{1}{a} & 0 & 0 \\ -\frac{b}{ac} & \frac{1}{c} & 0 \\ \frac{bd}{ace} & -\frac{d}{ce} & \frac{1}{e} \end{bmatrix} \quad \textbf{(14)}$$

Therefore, substitute (17) and (12) in $R_n=\rho(AB^{-1})$, so we have

$$R_n = \begin{bmatrix} 0 & \rho_1 S & \rho_2 S \\ 0 & 0 & 0 \\ 0 & 0 & 0 \end{bmatrix} \begin{bmatrix} \frac{1}{a} & 0 & 0 \\ -\frac{b}{ac} & \frac{1}{c} & 0 \\ \frac{bd}{ace} & -\frac{d}{ce} & \frac{1}{e} \end{bmatrix} \quad \textbf{(15)}$$

$$R_n = \frac{-b\rho_1 S}{ac} + \frac{bd\rho_2 S}{ace}$$

$$R_n = R_1 + R_2$$

Where $R_1=\frac{-b\rho_1 S}{ac}$ and $R_2=\frac{bd\rho_2 S}{ace}$

Substituting these values into the equation above:

$a=(\tau+\mu)$; $b=-\tau$; $c=(a\gamma+(1-a)\gamma+\mu+\delta_1)$; $d=-\delta_1$; and $e=(\mu_p+\eta-\xi)$, we get

$$R_n = \frac{\tau(1-\phi)\Gamma}{\mu(\tau+\mu)(a\gamma+(1-a)\gamma+\mu+\delta_1)}\left(\rho_1 + \frac{\delta_1\rho_2}{(\mu_p+\eta-\xi)}\right) \quad (16)$$

Moreover, let R_1 and R_2 denote the respective contributions stemming from direct and indirect transmissions, respectively.

2.4 Stability Property

2.4.1 Local stability of the disease-free steady-state

In this examination, we investigate the regional robustness of the equilibrium devoid of disease. This characteristic delves into the temporal evolution of the model's parameters when the virus is absent, indicating the equilibrium devoid of disease. It facilitates comprehension of the model's dynamics in the absence of the virus and its sensitivity to minor alterations or disturbances.

Theorem 1:

Within the domain of model system (2), the disease-free equilibrium is regarded as locally asymptotically stable (LAS) provided that all eigenvalues of the associated Jacobian matrix exhibit negative real components.

Proof:

To clarify the aforementioned theorem, we proceed with the calculation of the Jacobian matrix concerning the dynamics of the system at the state of disease-free equilibrium (DFE). The Jacobian matrix, represented by $J(S, V, L, A, T, R, P)$, facilitates the determination and estimation of the eigenvalues of the system. The Jacobian matrix is expressed as follows:

$$J = \begin{bmatrix} -\sigma+\mu & 0 & 0 & \rho_1 S & 0 & 0 & \rho_2 S \\ \sigma & -\mu & 0 & 0 & 0 & 0 & 0 \\ 0 & 0 & -(\tau+\mu) & 0 & 0 & 0 & 0 \\ 0 & 0 & \tau & -(a\gamma+(1-a)\gamma+\mu+\delta_2) & 0 & 0 & 0 \\ 0 & 0 & 0 & (1-a)\gamma & -(\theta_2+\mu+\delta_2) & 0 & 0 \\ 0 & 0 & 0 & a\gamma & \theta_2 & -\mu & 0 \\ 0 & 0 & 0 & \delta_1 & 0 & \delta_2 & -(\mu_p+\eta-\xi) \end{bmatrix} \quad (17)$$

Now, we calculate the eigenvalue, $|J-\lambda I|=0$, where λ represents our eigenvalue.

$$|J-\lambda I|=\begin{vmatrix} -(\mu-\sigma)-\lambda & 0 & 0 & \rho_1 S & 0 & 0 & \rho_2 S \\ \sigma & -\mu-\lambda & 0 & 0 & 0 & 0 & 0 \\ 0 & 0 & -(\tau+\mu)-\lambda & 0 & 0 & 0 & 0 \\ 0 & 0 & \tau & -(a\gamma+(1-a)\gamma+\mu+\delta_2)-\lambda & 0 & 0 & 0 \\ 0 & 0 & 0 & (1-a)\gamma & -(\theta_2+\mu+\delta_2)-\lambda & 0 & 0 \\ 0 & 0 & 0 & a\gamma & \theta_2 & -\mu-\lambda & 0 \\ 0 & 0 & 0 & \delta_1 & 0 & \delta_2 & -(\mu_p+\eta-\xi)-\lambda \end{vmatrix} \quad \textbf{(18)}$$

The eigenvalues of matrix $J(S, V, L, A, T, R, P)$, as depicted in the provided matrix, serve as crucial indicators of system dynamics. It is evident that these eigenvalues solely consist of real values, without any presence of imaginary components. The indication of these eigenvalues holds significant epidemiological ramifications, particularly when assessing the stability of the Disease-Free Equilibrium (DFE). Notably, in this context, all eigenvalues exhibit negative real components, affirming the local asymptotic stability of the model at the DFE.

2.4.2 Analysis of global stability of disease-free equilibrium (DFE)

Theorem 4:

The globally asymptotically stable non-negative equilibrium point of model (2) is guaranteed to be attained under conditions where $G^0 > 1$.

V,

Proof:

In order to assess the worldwide stability of this equilibrium E^0, we construct the ensuing Lyapunov function employing the specified approach.

$$\begin{aligned} &G(S,V,L,A,T,R,P)= \\ &\left(S-S^0-S^0\log\frac{S^0}{S}\right)+\left(V-V^0-V^0\log\frac{V^0}{V}\right)+\left(L-L^0-L^0\log\frac{L^0}{L}\right) \\ &+\left(A-A^0-A^0\log\frac{A^0}{A}\right)+\left(T-T^0-T^0\log\frac{T^0}{T}\right)+\left(P-P^0-P^0\log\frac{P^0}{p}\right) \end{aligned} \quad \textbf{(19)}$$

The derivative of G along the solution path of (2) can be obtained through direct calculation as follows:

$$\frac{dG}{dt}=\left(\frac{S-S^0}{S}\right)+\left(\frac{V-V^0}{V}\right)+\left(\frac{L-L^0}{L}\right)+\left(\frac{A-A^0}{A}\right)+\left(\frac{T-T^0}{T}\right)+\left(\frac{R-R^0}{R}\right) \quad (20)$$

We proceed to extend the aforementioned equation and partition it into distinct positive and negative components. Let the positive term be symbolized as P_t, and the negative term as N_t. Consequently, we derive:

$$\frac{dG}{dt}=P_t-N_t$$

$$S=\left(1-\frac{S^0}{S}\right)(\omega+\sigma+\mu)+\left(1-\frac{V^0}{V}\right)\mu+\left(1-\frac{L^0}{L}\right)(\tau+\mu)+\left(1-\frac{A^0}{A}\right)(a\gamma+(1-a)\gamma+\mu+\delta_1)+\left(1-\frac{T^0}{T}\right)(\theta_2+\mu+\delta_2)+\left(1-\frac{P^0}{P}\right)(\mu_p+\eta-\xi) \quad (21)$$

Similarly,

$$E=\frac{(S-S^0)^2}{S}(\phi_2+\mu_P)+\frac{(V-V^0)^2}{V}(\theta_1+\theta_1+\mu_P)+\frac{(L-L^0)^2}{L}(\mu_P+\delta_P+(1-\alpha_1)\theta_4+\alpha_1\theta_3)+\frac{(A-A^0)^2}{A}(\mu_P+\delta_P+\alpha_2)+\frac{(T-T^0)^2}{T}(\mu_P+\delta_P+\theta_5)+\frac{(P-P^0)^2}{P}(\phi_1+\mu_H) \quad (22)$$

Given the condition that $P_t < N_t$, it follows that $\frac{dG}{dt}$ will exhibit negativity definiteness along the trajectory of the solution space of the system. Consequently, this implies that exclusively at the Disease-Free Equilibrium (E0), $\frac{dG}{dt}\leq 0$ will hold. This observation suggests the global stability of the system at the Disease-Free Equilibrium

2.4.3 The presence of the endemic equilibrium points

In this investigation, we delve into the analysis of endemic equilibrium configurations, denoting stable solutions inherent to the model, wherein Hepatitis A and E endure within the populace perpetually. These equilibrium points denote the

steady disease states where the number of infected individuals and other compartments stabilizes.

The endemic equilibrium points are defined as $\left(S^*(t), 0, 0, 0, 0, 0, 0\right)$ that satisfy $S' = V' = L' = A' = T' = R' = P' = 0$. By setting equation (2) to 0, we have

$$\left.\begin{aligned} 0 &= (1-\phi)\Gamma - (\omega+\sigma+\mu)S^* \\ 0 &= \phi\Gamma + \sigma S^* - \mu V^* \\ 0 &= \omega S^* - (\tau+\mu)L^* \\ 0 &= \tau L^* - (a\gamma + (1-a)\gamma + \mu + \delta_1)A^* \\ 0 &= (1-a)\gamma A^* - (\theta_2 + \mu + \delta_2)T^* \\ 0 &= a\gamma A^* + \theta_2 T^* - \mu R^* \\ 0 &= \delta_1 A^* + \delta_2 R^* - (\mu_p + \eta - \xi)P^* \end{aligned}\right\} \quad \textbf{(23)}$$

Where $\omega = \rho_1 A + \rho_2 P$

$$S^* = \frac{(1-\phi)\Gamma}{(\omega+\sigma+\mu)};\ V^* = \frac{(\phi\Gamma+\sigma)(1-\phi)\Gamma}{\mu(\omega+\sigma+\mu)};\ L^* = \frac{\omega(1-\phi)\Gamma}{(\tau+\mu)(\omega+\sigma+\mu)}$$

$$A^* = \frac{\tau\omega(1-\phi)\Gamma}{(a\gamma+(1-a)\gamma+\mu+\delta_1)(\tau+\mu)(\omega+\sigma+\mu)};$$

$$T^* = \frac{(1-a)\gamma\tau\omega(1-\phi)\Gamma}{(\theta_2+\mu+\delta_2)(a\gamma+(1-a)\gamma+\mu+\delta_1)(\tau+\mu)(\omega+\sigma+\mu)};$$

$$R^* = \frac{a\gamma\tau\omega(1-\phi)\Gamma}{\mu(a\gamma+(1-a)\gamma+\mu+\delta_1)(\tau+\mu)(\omega+\sigma+\mu)} + \frac{\theta_2(1-a)\gamma\tau\omega(1-\phi)\Gamma}{\mu(\theta_2+\mu+\delta_2)(a\gamma+(1-a)\gamma+\mu+\delta_1)(\tau+\mu)(\omega+\sigma+\mu)} \quad \textbf{(24)}$$

$$P^* = \frac{1}{(\mu_p+\eta-\xi)}\left(\begin{aligned} &\delta_1\left(\frac{\tau\omega(1-\phi)\Gamma}{(a\gamma+(1-a)\gamma+\mu+\delta_1)(\tau+\mu)(\omega+\sigma+\mu)}\right) \\ &+\delta_2\left(\begin{aligned} &\frac{a\gamma\tau\omega(1-\phi)\Gamma}{\mu(a\gamma+(1-a)\gamma+\mu+\delta_1)(\tau+\mu)(\omega+\sigma+\mu)} \\ &+\frac{\theta_2(1-a)\gamma\tau\omega(1-\phi)\Gamma}{\mu(\theta_2+\mu+\delta_2)(a\gamma+(1-a)\gamma+\mu+\delta_1)(\tau+\mu)(\omega+\sigma+\mu)} \end{aligned}\right) \end{aligned}\right)$$

Employing conventional methodologies, the model demonstrates disease-free dynamics at equilibrium point E^0.

2.5 Sensitivity Analysis of the Model

This section focuses on performing a sensitivity analysis of the model, wherein the impact of parameter fluctuations on model prognostications is investigated. The aim is to identify significant parameters, elucidate their impact, and enhance the model's robustness.

In sensitivity analysis, a comprehensive exploration is conducted wherein parameters are systematically varied within their respective feasible ranges, while meticulously observing the consequent dynamics of the model. Such variation can be executed either in isolation (commonly denoted as one-at-a-time sensitivity analysis) or collectively (referred to as global sensitivity analysis) for multiple parameters concurrently.

We conducted an assessment of the model's reproductive ratio R_n to evaluate variations and the impact of parameter alterations (Table 2) and the results graphically displaced in figure 2.

2.5.1 Definition

The elucidation of the Normalized Forward-Sensitivity Index concerning variable V, dependent on parameter U, is expounded upon as follows:

$$X_U^V = \frac{\partial V}{\partial U} \cdot \frac{U}{V} \tag{25}$$

In reference to the model parameters, we shall undertake the computation of sensitivity indices pertaining to the basic reproductive ratio, designated as R_n.

2.5.2 Sensitivity index for Γ

The calculated metric denoted as the Normalized Forward-Sensitivity Index for λ is expressed as:

$$X_\Gamma^{R_n} = \frac{\partial R_n}{\partial \Gamma} \cdot \frac{\Gamma}{R_n} \tag{26}$$

$$R_n = \frac{\tau(1-\phi)\Gamma}{\mu(\tau+\mu)(a\gamma+(1-a)\gamma+\mu+\delta_1)}\left(\rho_1+\frac{\delta_1\rho_2}{(\mu_p+\eta-\xi)}\right)$$

Evaluating the derivatives in equation (43), we obtain:

$$\frac{\partial R_n}{\partial \Gamma} = \frac{1}{\Gamma}R_n \tag{27}$$

Then,

$$X_{\Gamma}^{R_n} = \frac{\partial R_n}{\partial \Gamma}.\frac{\Gamma}{R_n} = \frac{1}{\Gamma}R_n.\frac{\Gamma}{R_n}$$

$$\therefore X_{\Gamma}^{R_n} = +1 \tag{28}$$

This gives us the sensitivity index Γ.

The sensitivity analyses for the remaining parameters contributing to the basic reproductive ratio are conducted using a standardized methodology, ensuring uniformity in the computational process. Consequently, the sensitivity measures for these parameters are delineated as follows:

Table 2*. Indices of sensitivity regarding additional parameters within the framework of the basic reproductive rate are assessed.*

Variables	Values	Index indicator
ϕ	-0.6666667	-
Γ	1	+
ρ_1	0.5238095238	+
ρ_2	0.4761904762	+
μ	-1.081097152	-
τ	0.07918968688	+
a	0.00000	+
γ	-0-1108991705	-
δ_1	-0.4110028875	-
μ_p	-0.2245670995	-
η	-0.4491341991	-
ξ	0.1975108225	+

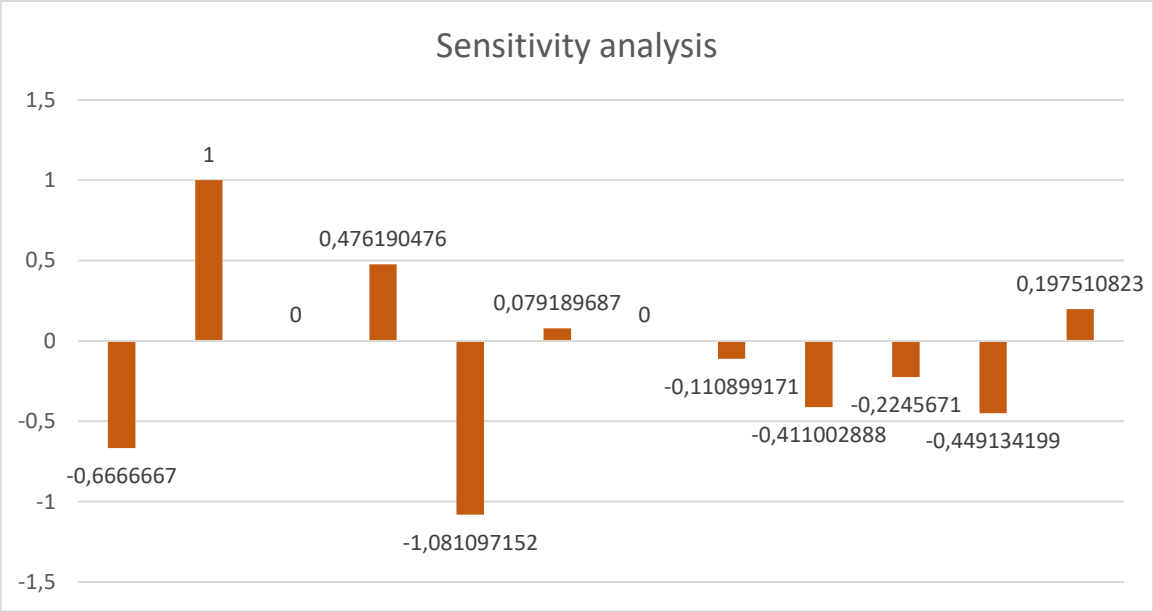

***Figure 2**. Sensitivity analysis.*

2.5.3 Interpretation of sensitivity analysis

A sensitivity index with a negative value signifies an inverse correlation between the parameter R_n (Table 2). Conversely, a sensitivity index with a positive value indicates that an increment in the parameter value results in a corresponding elevation in R_n. This analytical approach aids in discerning the parameters exerting significant influence on the outcomes of our analysis.

2.6 Optimal Strategies for Controlling the Model

The aim is to curtail disease transmission and its repercussions, considering resource constraints and optimizing the implementation of available interventions. These strategies typically entail a blend of preventive measures, surveillance, vaccination initiatives, and prompt case management. Several key components contribute to effective hepatitis control measures. These encompass adjusting transmission dynamics by lowering transmission rates through interventions such as health education $(1-\vartheta_1)$ campaigns, where ϑ_1 denotes health education and awareness. These public health endeavors raise awareness about hepatitis A and E transmission routes and preventive measures, thereby empowering individuals and communities to safeguard against infection. Vaccination campaigns target susceptible individuals (ϑ_2), while treatment efforts focus on acute cases (ϑ_3).

Sanitation initiatives (ϑ_4) address the removal of pathogens, further contributing to disease control. Building upon these foundations, we formulate a set of novel equations:

Building upon these premises, we formulate the following set of novel equations:

$$\left.\begin{aligned}
\frac{dS}{dt} &= (1-\phi)\Gamma - \left((1-\vartheta_1)(\rho_1 A + \rho_2 P) + \vartheta_2 + \mu\right)S \\
\frac{dV}{dt} &= \phi\Gamma + \vartheta_2 S - \mu V \\
\frac{dL}{dt} &= (1-\vartheta_1)(\rho_1 A + \rho_2 P)S - (\tau + \mu)L \\
\frac{dA}{dt} &= \tau L - \left(a\vartheta_3 + (1-a)\vartheta_3 + \mu + \delta_1\right)A \\
\frac{dT}{dt} &= (1-a)\vartheta_3 A - (\theta_2 + \mu + \delta_2)T \\
\frac{dR}{dt} &= a\vartheta_3 A + \theta_2 T - \mu R \\
\frac{dP}{dt} &= \delta_1 A + \delta_2 R - \left(\mu_p + \vartheta_4 - \xi\right)P
\end{aligned}\right\} \quad \textbf{(29)}$$

2.7 Examination of the Model Integrating Preventive Interventions

In this segment, we have developed a structured model, placing significant focus on leveraging Pontryagin's Maximum Principle for potential manipulation. Emphasizing the optimal solution delineated in equation set (29), a significant concern related to control has been identified and subsequently expounded upon before embarking on its comprehensive global optimization. The intricate process of selecting the most effective strategies is encapsulated by the objective function represented as F. The primary objective is to minimize the population susceptible to, exposed to, and affected by the disease, covering both asymptomatic and symptomatic cases, over a specified time interval [0, T].

Let $W = \{(\vartheta_1, \vartheta_2, \vartheta_3, \vartheta_4) \in W\}$ define over a Lebesgue measurable set on $[0,1]$

For $0 \le \vartheta_i(t) \le 1 \in [0,1], i = 1, 2, 3, 4$

Subsequently, the establishment of the objective function, designated as G, is undertaken.

$$G(\vartheta_1,\vartheta_2,\vartheta_3,\vartheta_4)=\int_0^T\left(Q_1L+Q_2V+Q_3T+Q_4P+\frac{1}{2}\left(V_1\vartheta_1^{\,2}+V_2\vartheta_2^{\,2}+V_3\vartheta_3^{\,2}+V_4\vartheta_4^{\,2}\right)\right)dt \qquad \textbf{(30)}$$

Constraint to

$$\left.\begin{aligned}
\frac{dS}{dt}&=(1-\phi)\Gamma-\left((1-\vartheta_1)(\rho_1A+\rho_2P)+\vartheta_2+\mu\right)S\\
\frac{dV}{dt}&=\phi\Gamma+\vartheta_2S-\mu V\\
\frac{dL}{dt}&=(1-\vartheta_1)(\rho_1A+\rho_2P)S-(\tau+\mu)L\\
\frac{dA}{dt}&=\tau L-\left(a\vartheta_3+(1-a)\vartheta_3+\mu+\delta_1\right)A\\
\frac{dT}{dt}&=(1-a)\vartheta_3A-(\theta_2+\mu+\delta_2)T\\
\frac{dR}{dt}&=a\vartheta_3A+\theta_2T-\mu R\\
\frac{dP}{dt}&=\delta_1A+\delta_2R-\left(\mu_p+\vartheta_4-\xi\right)P
\end{aligned}\right\} \qquad \textbf{(31)}$$

The parameter denoting the final time point is represented by T, with coefficients Q_1 through Q_4 signifying the weight coefficients assigned to the virus across various demographic categories, including latent classes, vaccinated individuals, treatment of acute individuals, and pathogens.

The primary focus of this section is to reduce operational costs, as outlined in equation (30). Additionally, our investigation extends to encompass an analysis of the social and economic implications $V_1\vartheta_1^{\,2}, V_2\vartheta_2^{\,2}, V_3\vartheta_3^{\,2}$, and $V_4\vartheta_4^{\,2}$ linked to the outlined scenario.

In pursuit of addressing the control challenge, our endeavors are aimed at understanding the functionalities.

$\left(\vartheta_1^{\,*}(t),\vartheta_2^{\,*}(t),\vartheta_3^{\,*}(t),\vartheta_4^{\,*}(t)\right)$ such that

$$G\left(\vartheta_1^{\,*}(t),\vartheta_2^{\,*}(t),\vartheta_3^{\,*}(t),\vartheta_4^{\,*}(t)\right)=\min\left\{G(\vartheta_1,\vartheta_2,\vartheta_3,\vartheta_4),(\vartheta_1,\vartheta_2,\vartheta_3,\vartheta_4)\in W\right\} \qquad \textbf{(32)}$$

2.7.1 The presence of an optimal control solution

Theorem:

Following equation (30), it is crucial to examine $G(\vartheta_1, \vartheta_2, \vartheta_3, \vartheta_4)$ within the constraints specified in (31), with t=0 representing the initial condition. Thus, in determining the optimal control, ensuring the aforementioned condition to be $\vartheta^* = \vartheta_1^*(t), \vartheta_2^*(t), \vartheta_3^*(t), \vartheta_4^*(t)$ is imperative.

$$G\left(\vartheta_1^*(t), \vartheta_2^*(t), \vartheta_3^*(t), \vartheta_4^*(t)\right) = \min\left\{G(\vartheta_1, \vartheta_2, \vartheta_3, \vartheta_4), (\vartheta_1, \vartheta_2, \vartheta_3, \vartheta_4) \in W\right\}$$

Proof:

Due to the convexity exhibited by the integrand G regarding control measures $\vartheta_1, \vartheta_2, \vartheta_3, \vartheta_4$, the presence of an optimal control solution is guaranteed.

Subsequently, it is crucial to elucidate the most effective remedy. The Lagrangian function is formulated as follows:

$$L = Q_1 L + Q_2 V + Q_3 T + Q_4 P + \frac{1}{2}\left(V_1 \vartheta_1^{\,2} + V_2 \vartheta_2^{\,2} + V_3 \vartheta_3^{\,2} + V_4 \vartheta_4^{\,2}\right) \tag{33}$$

The Hamiltonian function is given as;

$$\begin{aligned}
\Pi &= Q_1 L + Q_2 V + Q_3 T + Q_4 P + \frac{1}{2}\left(V_1 \vartheta_1^{\,2} + V_2 \vartheta_2^{\,2} + V_3 \vartheta_3^{\,2} + V_4 \vartheta_4^{\,2}\right) \\
&+ \Omega_S\left[(1-\phi)\Gamma - \left((1-\vartheta_1)(\rho_1 A + \rho_2 P) + \vartheta_2 + \mu\right)S\right] \\
&+ \Omega_V\left[\phi\Gamma + \vartheta_2 S - \mu V\right] \\
&+ \Omega_L\left[(1-\vartheta_1)(\rho_1 A + \rho_2 P)S - (\tau + \mu)L\right] \\
&+ \Omega_A\left[\tau L - (a\vartheta_3 + (1-a)\vartheta_3 + \mu + \delta_1)A\right] \\
&+ \Omega_T\left[(1-a)\vartheta_3 A - (\theta_2 + \mu + \delta_2)T\right] \\
&+ \Omega_R\left[a\vartheta_3 A + \theta_2 T - \mu R\right] \\
&+ \Omega_P\left[\delta_1 A + \delta_2 R - (\mu_p + \vartheta_4 - \xi)P\right]
\end{aligned} \tag{34}$$

Given $\Omega_k, k \in \{S, V, L, A, T, R, P\}$ are distinct and non-overlapping variables.

Currently, we are poised to implement the requisite variables into the Hamiltonian Π for thorough examination.

In our pursuit of clarifying the adjoint equation and satisfying the transversality condition, we employ the Hamiltonian function Π as our analytical

instrument. Through differential calculus, we ascertain the derivatives of the variables S,V,L,A,T,R,P relative to the Hamiltonian. This methodical process results in the derivation of the adjoint equation, as presented below:

$$\begin{aligned}
\frac{d\Omega_S}{dt} &= -\frac{\partial \Pi}{dS} = \begin{bmatrix} \Omega_S\left[\left((1-\vartheta_1)(\rho_1 A+\rho_2 P)+\vartheta_2+\mu\right)\right]-\Omega_V\left[\vartheta_2\right] \\ -\Omega_L\left[(1-\vartheta_1)(\rho_1 A+\rho_2 P)\right] \end{bmatrix} \\
\frac{d\Omega_V}{dt} &= \frac{-\partial \Pi}{dV} = \left[-Q_2 V+\Omega_V[\mu]\right] \\
\frac{d\Omega_L}{dt} &= -\frac{\partial \Pi}{dL} = \left[\Omega_L\left[(\tau+\mu)\right]-\Omega_A[\tau]\right] \\
\frac{d\Omega_A}{dt} &= -\frac{\partial \Pi}{dA} = \begin{bmatrix} \Omega_S\left[(1-\vartheta_1)\rho_1 S\right]-\Omega_L\left[(1-\vartheta_1)\rho_1 S\right]+\Omega_A\left[(a\vartheta_3+(1-a)\vartheta_3+\mu+\delta_1)\right] \\ -\Omega_T\left[(1-a)\vartheta_3\right]-\Omega_R\left[a\vartheta_3\right]-\Omega_P\left[\delta_1\right] \end{bmatrix} \\
\frac{d\Omega_T}{dt} &= -\frac{\partial \Pi}{dT} = \left[-Q_3+\Omega_T\left[(\theta_2+\mu+\delta_2)\right]-\Omega_R\left[\theta_2\right]\right] \\
\frac{d\Omega_R}{dt} &= -\frac{\partial \Pi}{dR} = \left[\Omega_R[\mu]-\Omega_P\left[\delta_2\right]\right] \\
\frac{d\Omega_P}{dt} &= -\frac{\partial \Pi}{dP} = \left[-Q_4+\Omega_S\left[(1-\vartheta_1)\rho_2 S\right]-\Omega_L\left[(1-\vartheta_1)\rho_2 S\right]+\Omega_P\left[\left(\mu_p+\vartheta_4-\xi\right)P\right]\right]
\end{aligned} \tag{35}$$

Given the conditions of transversally to be $\Omega_k(T)=0, k\in\{S,V,L,A,T,R,P\}$.

In the quest for minimizing the Hamiltonian, symbolized as H, concerning the optimal control variables, we engage in the differentiation process with respect to $\vartheta_1,\vartheta_2,\vartheta_3,\vartheta_4$. This yields a set of equations, which we subsequently equate to zero to determine the optimal control configuration. This methodology culminates in the attainment of the desired optimal control solution.

With $S=S^*,V=V^*,L=L^*,A=A^*,T=T^*,R=R^*,P=P^*$

Then, we have

$$\begin{aligned}
\frac{d\Pi}{d\vartheta_1} &= V_1\vartheta_1^{\,*}-\left(\rho_1 A+\rho_2 P\right)S\left(\Omega_L-\Omega_S\right)=0 \\
\frac{d\Pi}{d\vartheta_2} &= V_2\vartheta_2^{\,*}-\left(\Omega_S-\Omega_V\right)S=0 \\
\frac{d\Pi}{d\vartheta_3} &= V_3\vartheta_3^{\,2}-(1-a)A\left(\Omega_A-\Omega_T\right)-aA\left(\Omega_A-\Omega_R\right)=0 \\
\frac{d\Pi}{d\vartheta_4} &= V_4\vartheta_4^{\,*}-\Omega_P P=0
\end{aligned} \tag{36}$$

By simplifying the expressions, we arrive at a solution for the optimal control strategy.

$$\begin{aligned}
\vartheta_1^* &= \frac{(\rho_1 A + \rho_2 P)S(\Omega_L - \Omega_S)}{V_1} \\
\vartheta_2^* &= \frac{(\Omega_S - \Omega_V)S}{V_2} \\
\vartheta_3^* &= \frac{(1-a)A(\Omega_A - \Omega_T) + aA(\Omega_A - \Omega_R)}{V_3} \\
\vartheta_4^* &= \frac{\Omega_P P}{V_4}
\end{aligned} \tag{37}$$

Applying the boundary conditions, the solution is provided as follows.

$$\begin{aligned}
\vartheta_1 &= \min\left\{1, \max\left\{0, \frac{(\rho_1 A + \rho_2 P)S(\Omega_L - \Omega_S)}{V_1}\right\}\right\}, \\
\vartheta_2 &= \min\left\{1, \max\left\{0, \frac{(\Omega_S - \Omega_V)S}{V_2}\right\}\right\}, \\
\vartheta_3 &= \min\left\{1, \max\left\{0, \frac{(1-a)A(\Omega_A - \Omega_T) + aA(\Omega_A - \Omega_R)}{V_3}\right\}\right\}, \\
\vartheta_4 &= \min\left\{1, \max\left\{0, \frac{\Omega_P P}{V_4}\right\}\right\}.
\end{aligned} \tag{38}$$

Proved.

3 RESULTS

3.1 Numerical Simulation

In this computational model, we present a method to analyze the temporal propagation of the ailment, fluctuations across various parameters, and the evaluation of intervention effects. This facilitates researchers and public health officials in gaining insights into disease behavior across diverse scenarios and evaluating the efficacy of various control strategies.

***Table 3**. Parameters with their values.*

Parameters	Values	Source
ϕ	0.4	S. E. Mwaijande et al. [2]
Γ	1000	S. E. Mwaijande et al. [2]
ϑ_1	0.99	Assumed
ρ_1	0.1	S. E. Mwaijande et al. [2]
ρ_2	0.2	S. E. Mwaijande et al. [2]
ϑ_2	0.9	Assumed
μ	0.00172	S. E. Mwaijande et al. [2]
τ	0.02	Assumed
a	0.02	Estimated
γ	0.1	Estimated
δ_1	0.8	Sholicah et al. [1]
θ_2	0.02	Estimated
δ_2	0.8	Sholicah et al. [1]
ϑ_3	0.5	Assumed
μ_p	0.83	S. E. Mwaijande et al. [2]
η	$2 \bullet \mu_p$	S. E. Mwaijande et al. [2]
ξ	0.73	S. E. Mwaijande et al. [2]

The state variables' initial conditions are as follows; $S(0) = 1500,\ E(0) = 1400,$ $I_A(0) = 880,\quad I_S(0) = 550,\quad Q(0) = 500,\quad I(0) = 800,$ and $R(0) = 1100$. The requisite parameter values essential for conducting the simulation are delineated within the confines of Table 3.

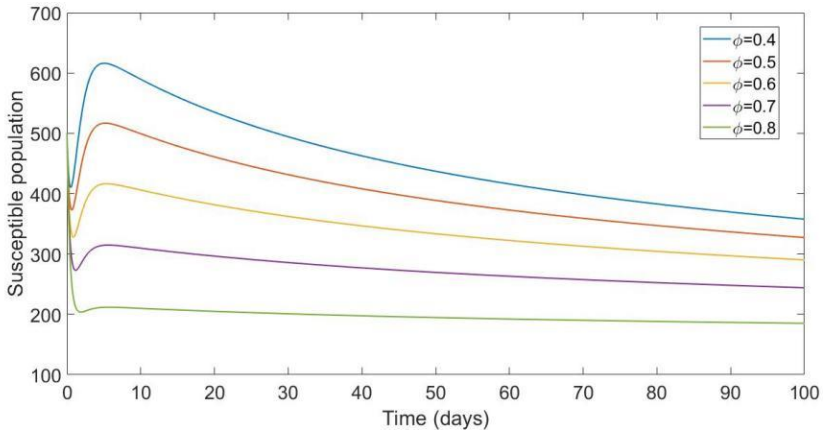

***Figure 3**. Variation of susceptible population with different phi values.*

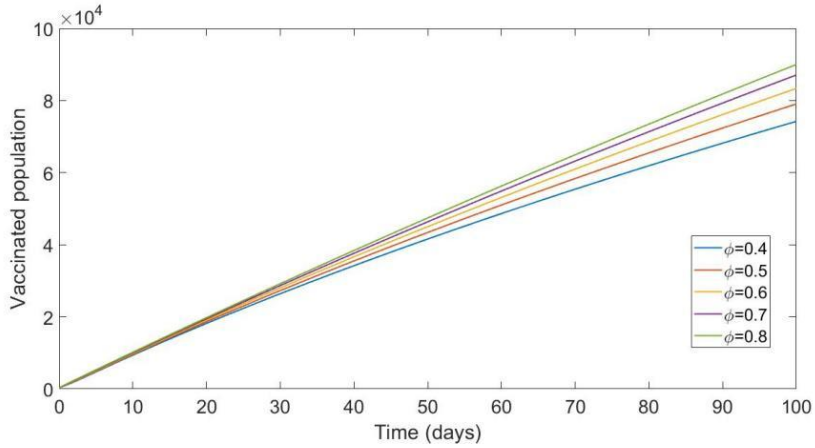

***Figure 4**. Variation of vaccinated population with different phi values.*

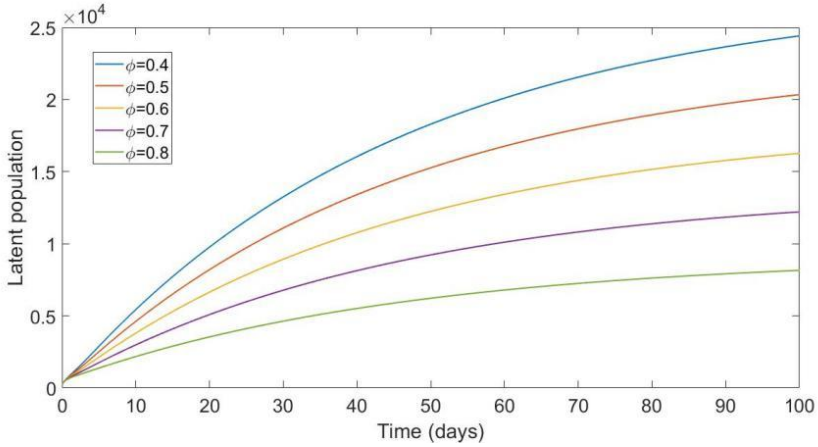

***Figure 5.** Variation of latent population with different phi values.*

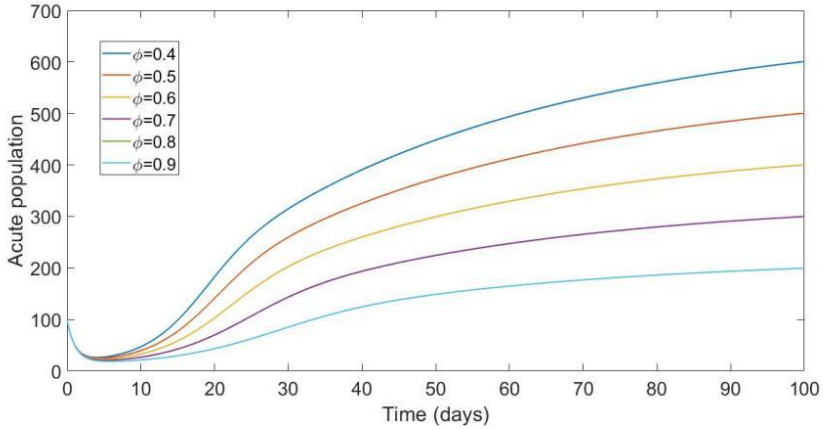

***Figure 6.** Variation of acute population with different phi values.*

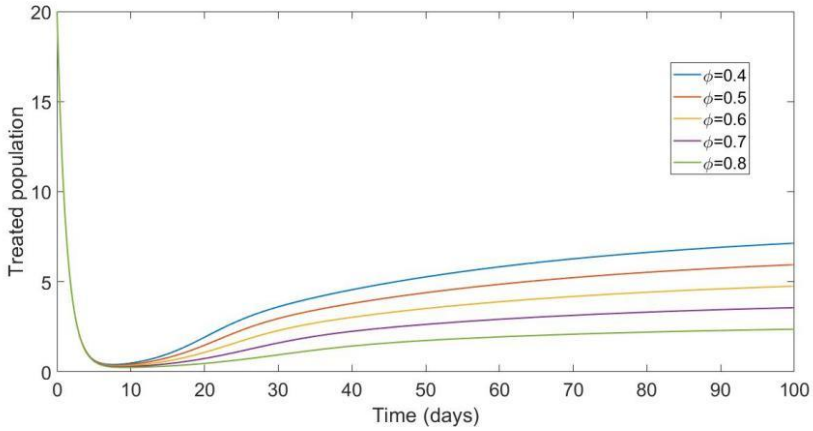

Figure 7. *Variation of treated population with different phi values.*

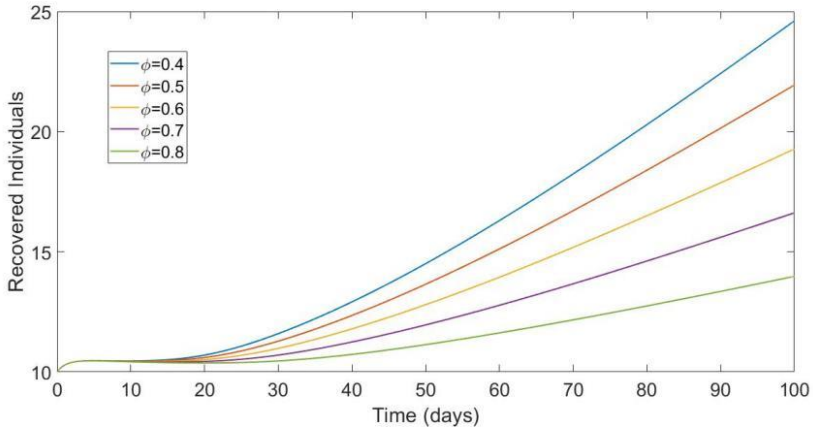

Figure 8. *Variation of recovered population with different phi values.*

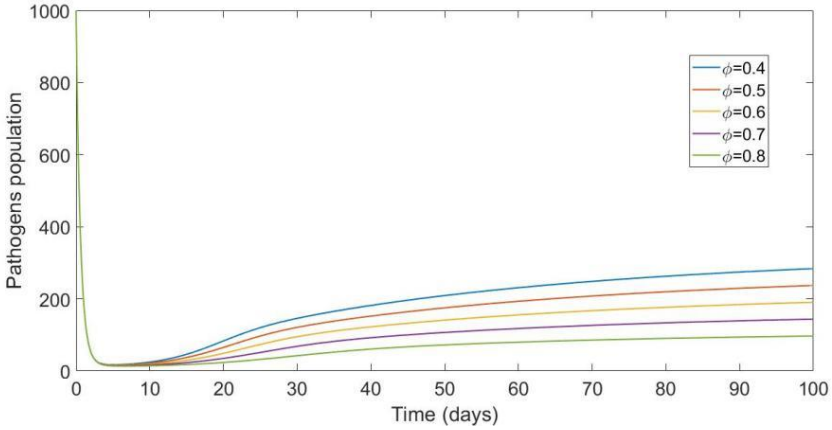

Figure 9. *Variation of pathogens population with different phi values.*

2. Figure 10 through Figure 12 shows the effect of the pathogens shed rate by the acute individuals in the water or food.

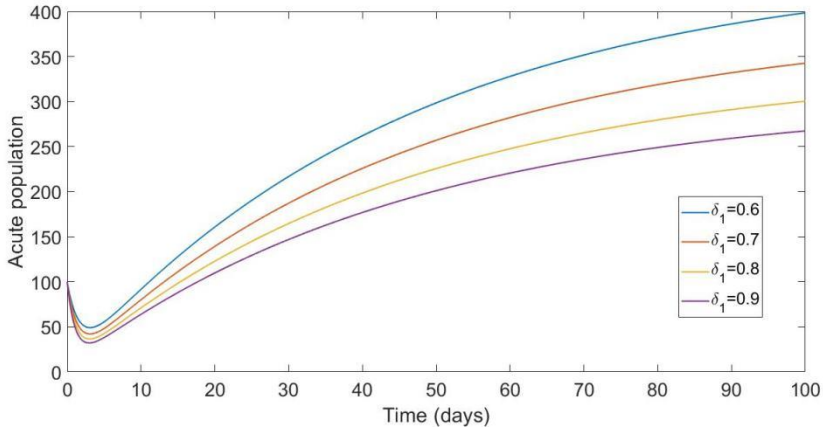

***Figure 10**. Variation of acute population with different shed rates.*

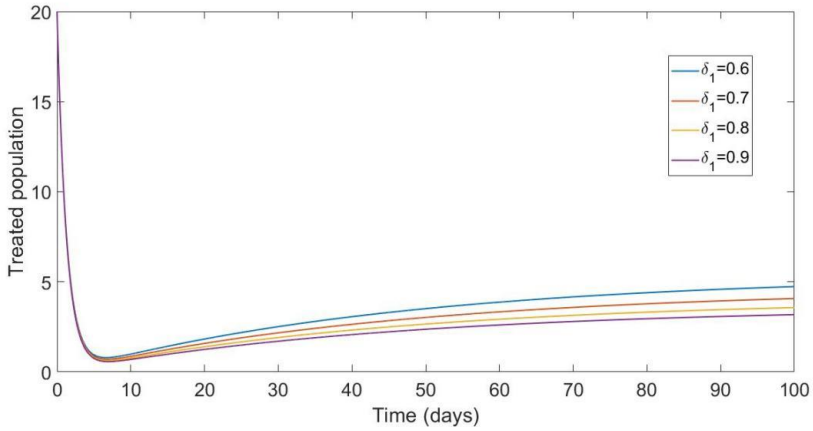

***Figure 11**. Variation of treated population with different shed rates.*

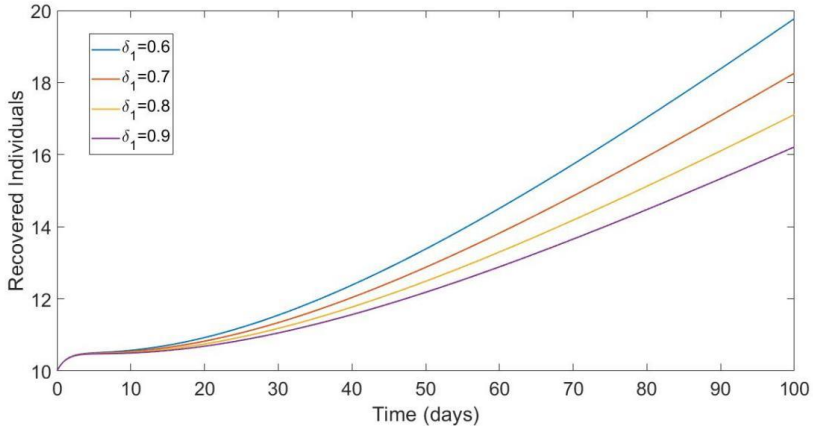

***Figure 12**. Variation of recovered population with different shed rates.*

3. Figure 13 through Figure 19 shows the effect of the control strategies on the population.

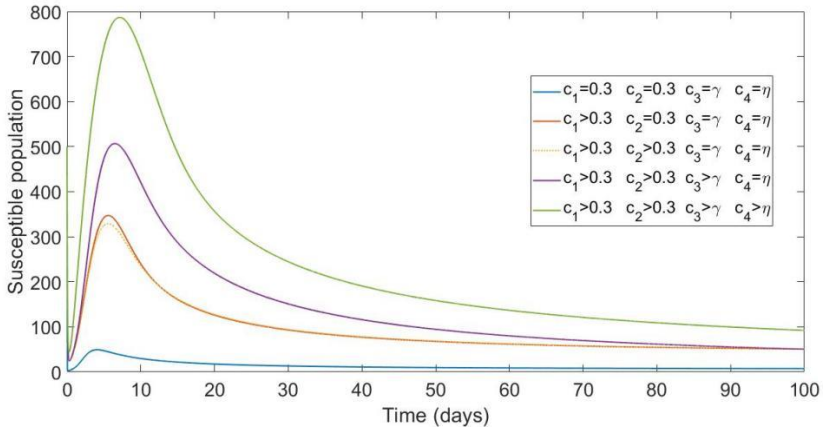

Figure 13*. Variation of susceptible population with control measures.*

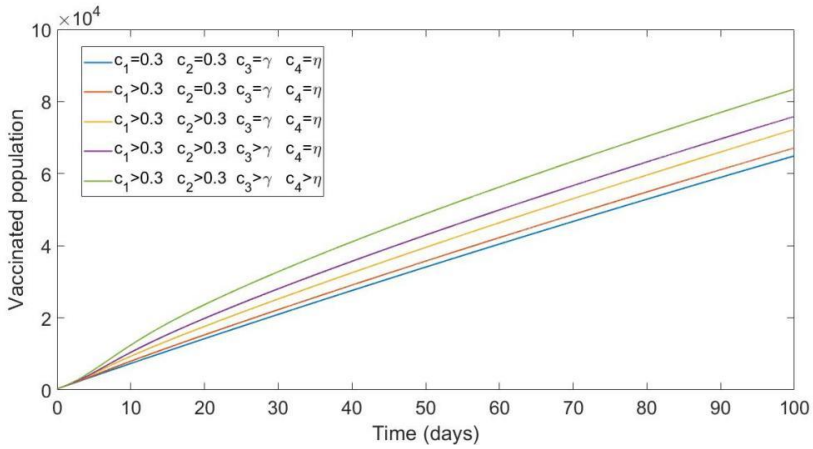

Figure 14*. Variation of vaccinated population with control measures.*

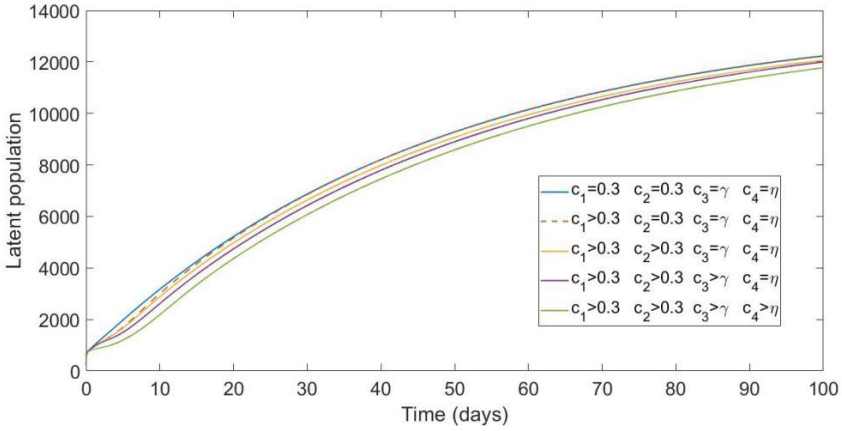

Figure 1 *Variation of latent population with control measures.*

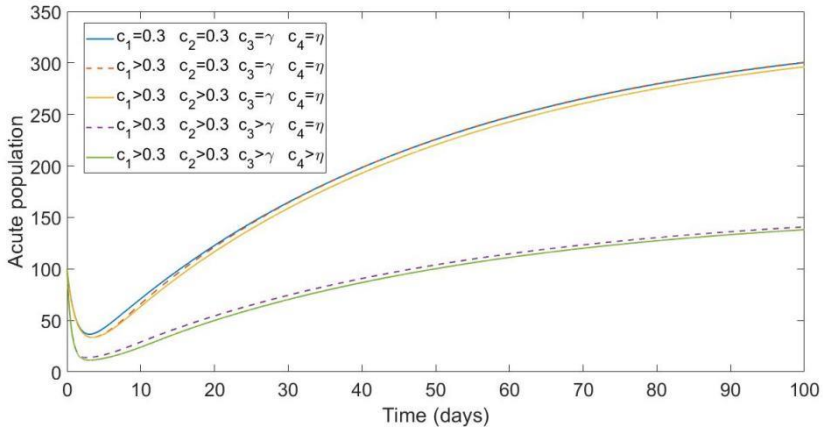

Figure 2 *Variation of acute population with control measures.*

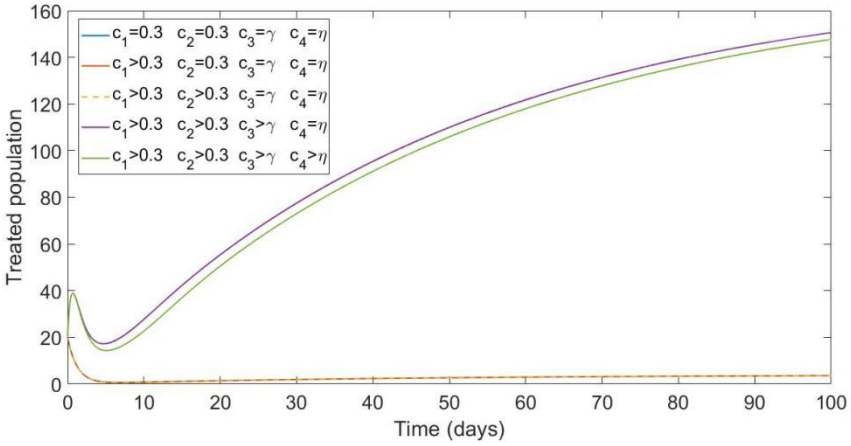

Figure 3*Variation of treated population with control measures.*

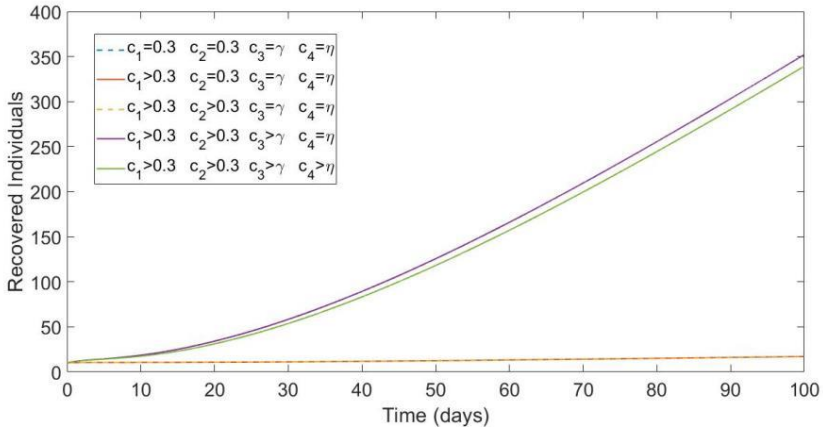

Figure 4*Variation of recovered population with control measures.*

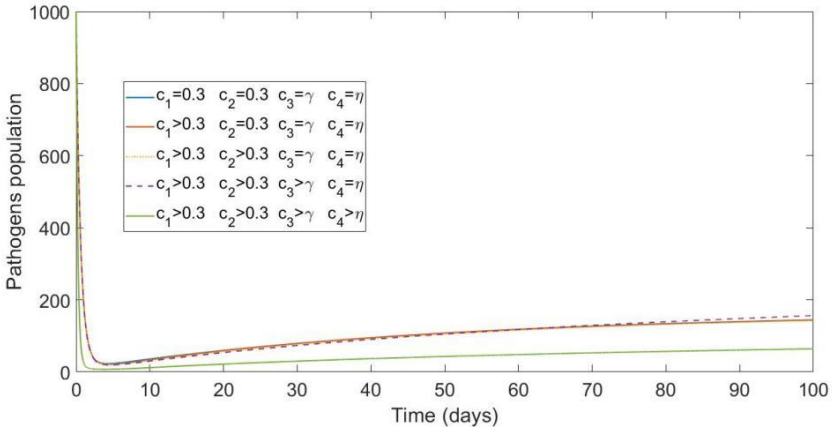

Figure 5*Variation of pathogens population with control measures.*

3.2 Discussion

Figure 3 depicts a decline in the susceptible population as the vaccination coverage increases. This trend aligns with expectations, as vaccination diminishes the pool of individuals vulnerable to infection. In Figure 4, the rise in the proportion of vaccinated susceptible corresponds with an uptick in the vaccinated population, indicating the efficacy of vaccination drives in augmenting the immunized cohort. Figure 5 illustrates a downturn in the latent population, suggesting the efficacy of vaccination in curbing the number of individuals exposed to infection but not yet symptomatic. This decline may signify either a direct impact of vaccination on transmission or an indirect effect stemming from the reduced pool of susceptible. Similarly, Figure 6 demonstrates that as the vaccination rate climbs, the count of individuals in the acute infection phase diminishes, hinting at vaccination's potential in mitigating the prevalence of actively infected individuals in the populace.

In Figure 7, the reduced incidence of acute infections due to vaccination results in fewer individuals necessitating treatment, implying that vaccination not only averts infection but also alleviates the strain on healthcare systems by decreasing the number of cases necessitating medical attention. Figure 8 showcases a decline in the recovered population, plausibly attributed to the reduction in the number of individuals contracting and subsequently recuperating from infections. This decline may stem from an overall reduction in infections owing to vaccination efforts. Moreover, Figure 9 reveals that the collective population of Hepatitis A and E pathogens within the community diminishes as vaccination diminishes the pool of

susceptible individuals available for transmission, thus constraining the diseases' spread.

Figure 10 illustrates a negative correlation between the rate of pathogen excretion and the population of actively infected individuals displaying clinical symptoms. This correlation suggests that an increase in pathogen excretion leads to a decrease in the number of individuals manifesting acute symptoms. Correspondingly, Figure 11 indicates a reduction in the count of acutely infected individuals undergoing treatment as pathogen excretion rises. Figure 12 implies a decline in the overall count of recovered individuals, despite some recovering from the infection, possibly due to a higher rate of new infections outpacing the rate of recovery. These observations indicate that elevated pathogen excretion by individuals in the acute stage contributes to diminishing counts of acute infections, treated cases, and ultimately, recoveries. This underscores the necessity of regulating pathogen transmission to mitigate the spread of infectious diseases such as Hepatitis A and E. In Figure 13, the susceptible population experiences a noticeable increase, likely attributed to heightened awareness campaigns leading to heightened case reporting or a more accurate estimation of the true susceptible population due to enhanced surveillance. Figure 14 illustrates the positive impact of targeted vaccination efforts in augmenting the vaccinated population, thereby reducing the pool of susceptible individuals over time. Simultaneously, Figure 15 depicts a decline in the latent population, indicating the efficacy of control measures in restraining the transmission dynamics of Hepatitis A and E. Health education initiatives are presumed to play a crucial role in shortening the duration of individuals in the latent stage by advocating for early detection and diagnosis.

Moreover, Figure 16 illustrates a consistent decrease in the acute population, indicative of successful intervention strategies. Vaccination campaigns and treatment efforts synergistically act to mitigate the burden of acute infections, thereby limiting the propagation of the disease within the population. However, Figures 17 and 18 show nuanced responses of the treated and recovered populations, respectively, to the different control strategies. While the implementation of health education, vaccination, and treatment leads to an increase in both populations, the emphasis on sanitation appears to yield a reduction. This observation underscores the importance of a multifaceted approach in disease control, wherein sanitation

efforts complement but do not replace other essential interventions aimed at treatment and prevention. Interestingly, Figure 19 reveals that the pathogen population experiences a significant reduction as control strategies intensify. This decline underscores the effectiveness of sanitation initiatives in mitigating environmental contamination and interrupting the transmission cycle of Hepatitis A and E. By targeting the removal of pathogens from water or food supplies, sanitation measures contribute substantially to disease control efforts.

Overall, findings underscore the transformative potential of multifaceted intervention strategies in taming Hepatitis A and E infections. Vaccination emerges as a cornerstone of disease control, reducing susceptibility and transmission rates. Concurrently, targeted treatment and health education initiatives bolster disease management and prevention efforts. Importantly, sanitation measures play a pivotal role in interrupting transmission cycles, mitigating environmental contamination, and enhancing overall disease control. This study represents a paradigm shift in public health dynamics, offering a holistic approach to infectious disease modeling and intervention design. By integrating mathematical modeling with real-world applications, this study provides actionable insights for policymakers, healthcare professionals, and public health practitioners. Findings herein pave the way for more effective, evidence-based strategies to combat Hepatitis A and E infections, ultimately advancing global health and well-being.

4 CONCLUSION

The analysis of the epidemiological dynamics of Hepatitis A and E infections demonstrates the critical importance of integrating diverse control strategies to mitigate the burden of these diseases on public health. This study highlights vaccination campaigns as a cornerstone for reducing the susceptible population, curtailing transmission, and alleviating pressure on healthcare systems. In tandem, health education initiatives play an essential role in fostering early detection, accurate diagnosis, and effective prevention, thereby curbing latent infections and empowering communities to adopt healthier behaviors.

The findings also underscore the efficacy of a multifaceted intervention framework, as reductions in acute infections and subsequent treatment needs

highlight the synergistic effects of combining vaccination, treatment, and health education. While vaccination directly reduces the number of actively infected individuals, it also indirectly decreases the healthcare burden by minimizing the demand for treatment and related resources. However, the nuanced responses of treated and recovered populations to different measures emphasize the necessity of a balanced approach. Specifically, sanitation efforts emerge as a pivotal component for reducing environmental contamination, interrupting pathogen transmission cycles, and complementing other strategies such as vaccination and treatment.

Future research should build upon this comprehensive framework by exploring the long-term implications of these strategies under varying epidemiological and environmental conditions. Key areas for further study include:

-Model refinement: Incorporating more complex variables such as regional disparities, climate change effects, and socioeconomic factors to enhance predictive accuracy.

- Cost-effectiveness analysis: Evaluating the economic feasibility of different intervention strategies to guide policymakers in resource allocation.

- Dynamic intervention design: Investigating adaptive strategies that respond to real-time epidemiological data for improved disease management.

- Pathogen evolution: Studying the impact of mutations in Hepatitis A and E viruses on the effectiveness of current interventions.

- Community resilience: Assessing the role of integrated interventions in improving population resilience against future outbreaks.

In summary, this study provides a robust framework for understanding and controlling Hepatitis A and E infections. By emphasizing the importance of a coordinated and evidence-based approach, it lays a strong foundation for future research and public health initiatives aimed at reducing disease burden and safeguarding global health.

Acknowledgement

The author appreciates the extraordinary input of Sunday Gbodogbe.

Statement of Research and Publication ethics.

The study is compiled within research and publications ethics.

Artificial Intelligence (AI) Contribution Statement

This manuscript was entirely written, edited, analyzed, and prepared without the assistance of any artificial intelligence (AI) tools. All content, including text, data analysis, and figures, was solely generated by the author.

REFERENCES

[1] M. Sholikah, C. Alfiniyah and Miswanto, "Stability analysis and optimal control of mathematical model for the spread of hepatitis E," *Commun. Math. Biol. Neurosci.*, vol. 37, pp. 1-24, 2020.

[2] S. E. Mwaijande and G. E. Mpogolo, "Modeling the Transmission Dynamics of Hepatitis A with Combined Vaccination and Sanitation Mitigation," *Comput. Math. Methods Med.*, pp. 1-19, 2023.

[3] WHO, *A. Hepatitis and World Health Organization*, 2022. [Online]. Available: http://www.who.int/mediacentre/factsheets/fs328/en/.

[4] MMWR, "Prevention of hepatitis A through active or passive immunization: Recommendations of the Advisory Committee on Immunization Practices (ACIP)," *MMWR Recomm. Rep.*, vol. 48, no. 12, pp. 1-37, 1999.

[5] J. T. Stapleton and S. M. Lemon, "Infectious Diseases," in *Hepatitis A and Hepatitis E*, Lippincott Co, Philadelphia, US, pp. 790-797, 1994.

[6] J. L. Trujillo-Ochoa, O. Viera-Segura, and N. A. Fiery, "Challenges in management of hepatitis A virus epidemiological transition in Mexico," *Ann. Hepatol.*, vol. 18, no. 1, pp. 14-22, 2019.

[7] C. J. Staes, T. L. Schlenker, I. Risk et al., "Sources of infection among persons with acute hepatitis A and no identified risk factors during a sustained community-wide outbreak," *Pediatrics*, vol. 106, no. 4, p. E54, 2000.

[8] E. Bianco, A. Mariano, A. Mele, E. Spada, and M. Tosti, "Epidemiology of acute viral hepatitis: twenty years of surveillance through SEIEVA in Italy and a review of the literature," *Rapporti Istisan*, vol. 12, 2006.

[9] R. Aggarwal and S. Naik, "Epidemiology of hepatitis E: current status," *J. Gastroenterol. Hepatol.*, vol. 24, no. 9, pp. 1484-1493, 2009.

[10] J. Zuckerman, "Hepatitis Viruses," in *Medical Microbiology*, 4th ed., S. Baron, Ed. Galveston, TX: Univ. Texas Med. Branch, 1996, ch. 70. [Online]. Available: https://www.ncbi.nlm.nih.gov/books/NBK7864

[11] G. J. Ebrahim, "The Five Hepatitis Viruses," *J. Trop. Pediatr.*, vol. 57, no. 6, pp. 401-404, 2011.

[12] D. K. Owens et al., "Screening for Hepatitis B Virus Infection in Pregnant Women: U.S. Preventive Services Task Force Reaffirmation Recommendation Statement," *JAMA*, vol. 322, no. 4, pp. 349-354, 2019.

[13] A. C. Loyinmi, and S. O. Gbodogbe, "Epidemiological viability and control of rotavirus: A mathematical modelling approach," *Fnaps journal*, vol. 6, no. 2, pp. 18-43, 2025.

[14] R. Ragusa, L. S. Corsaro, E. Frazzetto, E. Bertino, M. A. Bellia and G. Bertino, "Hepatitis C Virus Infection in Children and Pregnant Women," *AJP Rep.*, vol. 10, no. 1, pp. 121-127, 2020.

[15] S. Saab, R. Kullar, C. Amini and P. Gounder, “The next frontier: universal hepatitis C virus screening in pregnant women,” *Am. J. Obstet. Gynecol.*, 2020, doi:10.1016/j.ajog.2020.01.058.

[16] T. Ahmad, J. Hui, T. H. Musa, M. Behzadifar and M. Baig, “Seroprevalence of hepatitis E virus infection in pregnant women: a systematic review and meta-analysis,” *Ann. Saudi Med.*, vol. 40, no. 2, pp. 136–146, 2020.

[17] M. S. Khuroo, S. Kamili and M. S. Khuroo, “Clinical course and duration of viremia in vertically transmitted hepatitis E virus (HEV) infection in babies born to HEV-infected mothers,” *J. Viral Hepat.*, vol. 16, no. 7, pp. 519–523, 2009.

[18] WHO, “Hepatitis E,” WHO, 2018. [Online]. Available: https://www.who.int/news-room/fact-sheets/detail/hepatitis-e [Accessed: Aug. 29, 2018].

[19] G. S. Oluwafemi, and A.C. Loyinmi, “Model of optimal control strategies for the transmission of diphtheria,” *Journal of Information & Optimization Sciences* ISSN 0252-2667 (Print), ISSN 2169-0103 (Online). Available: https://tarupublication.s3.ap-south-1.amazonaws.com/articles/jios-1587.pdf DOI : 10.47974/JIOS-1587

[20] H. Sooryanarain and X. J. Meng, “Swine hepatitis E virus: Cross-species infection, pork safety and chronic infection,” *Virus Res.*, vol. 284, 197985, 2020. doi:10.1016/j.virusres.2020.197985

[21] H. Ren, J. Li, Z. Yuan, J. Hu, Y. Yu and Y. Lu, “The development of a combined mathematical model to forecast the incidence of hepatitis E in Shanghai, China,” *BMC Infect. Dis.*, vol. 13, no. 421, 2013.

[22] WHO, “Viral hepatitis,” WHO, 2010. [Online]. Available: http://apps.who.int/gb/ebwha/pdf_files/A62/A62_22-en.pdf

[23] N. Chitnis, J. M. Hyman and J. M. Cushing, “Determining important parameters in the spread of malaria through the sensitivity analysis of a mathematical model,” *Bull. Math. Biol.*, vol. 70, no. 5, 2008.

[24] C. Loyinmi and A. L. Ijaola, “Investigating the effects of some control measures on the dynamics of diphtheria infection using fractional order model,” *Math. Comput. Sci.*, vol. 5, no. 4, pp. 26–47, 2024. doi:10.30511/MCS.2024.2032110.1183

[25] Castillo-Chavez and B. Song, “Dynamical models of tuberculosis and their applications,” *Math. Biosci. Eng.*, vol. 1, no. 2, pp. 361–404, 2004.

[26] S. O. Gbodogbe, “Harmonizing epidemic dynamics: A fractional calculus approach to optimal control strategies for cholera transmission,” *Sci. Afr.*, vol. 27, 2025.

[27] Korobeinikov, “Global properties of infectious disease models with non-linear incidence,” *Bull. Math. Biol.*, vol. 69, no. 6, 2007.

[28] J. T. Stapleton and S. M. Lemon, “Infectious Diseases, (Chapter) Hepatitis A and Hepatitis E,” Lippincott Co, Philadelphia, US, pp. 790–797, 1994.

[29] K. Ayouni et al., “Hepatitis A virus infection in Central-West Tunisia: an age structured model of transmission and vaccination impact,” *BMC Infect. Dis.*, vol. 20, no. 1, pp. 1–13, 2020.

[30] F. Brouwer et al., “The impact of vaccination efforts on the spatiotemporal patterns of the hepatitis A outbreak in Michigan, 2016–18,” *Epidemiology*, vol. 31, no. 5, 2020.

[31] T. Van Effelterre, C. Marano and K. H. Jacobsen, “Modeling the hepatitis A epidemiological transition in Thailand,” *Vaccine*, vol. 34, no. 4, pp. 555–562, 2016.

[32] M. Ajelli, L. Fumanelli, P. Manfredi and S. Merler, “Spatiotemporal dynamics of viral hepatitis A in Italy,” *Theor. Popul. Biol.*, vol. 79, no. 1–2, pp. 1–11, 2011.

[33] M. Ajelli, M. Iannelli, P. Manfredi and M. L. C. degli Atti, “Basic mathematical models for the temporal dynamics of HAV in medium-endemicity Italian areas,” *Vaccine*, vol. 26, no. 13, pp. 1697–1707, 2008.

[34] A. C. Loyinmi, and S. O. Gbodogbe, "Mathematical modeling and control strategies for Nipah virus transmission incorporating bat-to-pig-to-human pathway," *EDUCATUM Journal of Science, Mathematics and Technology*, vol. 11, no. 1, pp. 54-80, 2024.

[35] E. Fiore, A. Wasley and B. P. Bell, "Prevention of hepatitis A through active or passive immunization: recommendations of the Advisory Committee on Immunization Practices (ACIP)," *MMWR Recomm. Rep.*, vol. 55, no. 7, 2006.

[36] T. P. Van Effelterre, T. K. Zink, B. J. Hoet, W. P. Hausdorff and P. A. Rosenthal, "Mathematical model of hepatitis A transmission in the United States indicates value of universal childhood immunization," *Clin. Infect. Dis.*, vol. 43, no. 2, pp. 158–164, 2006.

[37] M. A. D. Guimaraens and C. T. Codeço, "Experiments with mathematical models to simulate hepatitis A population dynamics under different levels of endemicity," *Cad. Saúde Pública*, vol. 21, no. 5, pp. 1531–1539, 2005.

[38] R. S. Koff, "Clinical manifestations and diagnosis of hepatitis A virus infection," *Vaccine*, vol. 10, no. Suppl. 1, pp. S15–S17, 1992.

[39] S. Krugman and J. P. Giles, "Viral hepatitis," *JAMA*, vol. 212, no. 6, pp. 1019–1029, 1970.

[40] C. J. Staes et al., "Sources of infection among persons with acute hepatitis A and no identified risk factors during a sustained community-wide outbreak," *Pediatrics*, vol. 106, no. 4, 2006.

[41] C. Loyinmi, S. O. Gbodogbe and K. O. Idowu, "On the interaction of the human immune system with foreign body: Mathematical modelling approach," *Kathmandu Univ. J. Sci. Eng. Technol.*, vol. 17, no. 2, pp. 1–17, 2023. [Online]. Available: https://journals.ku.edu.np/kuset/article/view/137

[42] K. M. Bisgard, A. Kao and J. Leake, "Haemophilus influenzae invasive disease in the United States, 1994–1995: near disappearance of a vaccine-preventable childhood disease," *Emerg. Infect. Dis.*, vol. 4, pp. 229–237, 1998.

[43] B. P. Bell, D. Kruszon-Moran and C. N. Shapiro, "Hepatitis A virus infection in the United States: serologic results from the third national health and nutrition examination survey," *Vaccine*, vol. 23, pp. 5798–5806, 2005.

[44] F. Averhoff, C. N. Shapiro and B. P. Bell, "Control of hepatitis A through routine vaccination of children," *JAMA*, vol. 286, pp. 2968–2973, 2001.

[45] R. Singh, P. Preeti and A. A. Raina, "Markovian epidemic queueing model with exposed, infection and vaccination based on treatment," *World Sci. News*, vol. 106, pp. 141–150, 2018.

[46] Din and Y. Li, "Optimizing HIV/AIDS dynamics: stochastic control strategies with education and treatment," *Eur. Phys. J. Plus*, vol. 139, no. 9, p. 812, 2024.

[47] S. M. A. Shah, H. Tahir, A. Khan and A. Arshad, "Stochastic model on the transmission of worms in wireless sensor network," *J. Math. Tech. Model.*, vol. 1, no. 1, pp. 75–88, 2024.

[48] Q. T. Ain, "Nonlinear stochastic cholera epidemic model under the influence of noise," *J. Math. Tech. Model.*, vol. 1, no. 1, pp. 52–74, 2024.

[49] Din, "Bifurcation analysis of a delayed stochastic HBV epidemic model: Cell-to-cell transmission," *Chaos Solitons Fractals*, vol. 181, 114714, 2024.

[50] S. Ullah, "Investigating a coupled system of Mittag-Leffler type fractional differential equations with coupled integral boundary conditions," *J. Math. Tech. Model.*, vol. 1, no. 2, pp. 16–28, 2024.